Electronic Supplementary Information (ESI)

Hierarchically porous metal-organic frameworks: rapid synthesis and enhanced gas storage performance

Chongxiong Duan,[a] Hang Zhang,[a] Feier Li,[a] Jing Xiao,[a] Shaojuan Luo,*[,b,d] and Hongxia Xi*[,a,c]

[a]*School of Chemistry and Chemical Engineering, South China University of Technology, Guangzhou 510640, China.*

[b]*Shenzhen Engineering Laboratory of Phosphorene and Optoelectronics, International Collaborative Laboratory of 2D Materials for Optoelectronic Science and Technology, Shenzhen University, Shenzhen 518060, China*

[c]*Guangdong Provincial Key Laboratory of Atmospheric Environment and Pollution Control, South China University of Technology, Guangzhou Higher Education Mega Centre, Guangzhou 510006, PR China*

[d]*Department of Chemical and Biological Engineering, The Hong Kong University of Science and Technology, Kowloon, Hong Kong*

Experimental Section

Chemicals. Copper nitrate trihydrate ($Cu(NO_3)_2 \cdot 3H_2O$), cupric chloride ($CuCl_2$), cupric acetate monohydrate ($Cu(AC)_2 \cdot H_2O$), 1,3,5-benzenetricarboxylic acid (H_3BTC), cobaltous nitrate hexahydrate ($Co(NO_3)_2 \cdot 6H_2O$), zinc nitrate hexahydrate ($Zn(NO_3)_2 \cdot 6H_2O$), 2-methylimidazole (2Im), imidazole-2-carboxyaldehyde (ICA), 1,4-butanediamine (BTDM, density 0.792 g/mL), tetramethyl-1,3-diaminopropane (TMPDA, density 0.78 g/mL), tetramethyldiaminomethane (TMDT, density 0.749 g/mL), succinic acid, succinonitrile, 1,4-dibromobutane, n-octane, dichlorobutane, 1,3-butadiene, and 1,2-butanediol, tetrabutylammonium chloride, tetrapropylammonium bromide, and *N, N*-dimethylformamide (DMF), above chemicals were purchased from J&K or aladdin Chemical Ltd, and utilized without further purification.

Synthesis of conventional HKUST-1 by a solvothermal method within 24 h at 110°C.

In a typical synthesis,[1] 2.5 mmol of 1,3,5-benzenetricarboxylic acid (H_3BTC) was added to 15 mL of ethanol to obtain solution A, and 4.5 mmol of copper nitrate trihydrate ($Cu(NO_3)_2 \cdot 3H_2O$) was

dispersed in 15 mL of deionized water to obtain solution B. After stirring for 30 min, solution A was added to solution B, and the mixture was stirred for 30 min more. The final gel mixture was transferred into a 100 mL Teflon-lined stainless steel autoclave stewing and heated to 110°C for 24 h. After cooling down, the solid product was filtered and washed with ethanol two times, then dried in an oven at 150°C for 12 h. The resulting product was denoted as C-HKUST-1.

Rapid room-temperature synthesis of hierarchically porous ZIF-67.

In a typical synthesis,[2] 0.655 g of cobaltous nitrate hexahydrate ($Co(NO_3)_2 \cdot 6H_2O$) and 0.167 g of 2-methylimidazole were dispersed in 20 mL of methanol solution at RTP. After stirring for 10 min, 0.82 mL of template BTDM was added to the mixture under fast magnetic stirring. After stirring for 1 min, the mixture was filtered and activated in ethanol solution four times at 60°C for a total duration of 48 h, then dried overnight in an oven at 120°C. The resulting product was denoted as H-ZIF-67_A1. The procedure used to synthesize H-ZIF-67_B1 was similar to the procedure used to prepare H-ZIF-67_A1, except that the template BTDM was replaced by TMPDA.

Rapid room-temperature synthesis of hierarchically porous ZIF-90.

2.0 mmol of zinc nitrate hexahydrate and 3.0 mmol of imidazole-2-carboxyaldehyde were dissolved in 30 mL of 2, 2-dinethyl butane, *N, N*-dimethylformamide (DMF). After stirring for 10 min, 0.33 mL of BTDM (2 mmol, molar ratio of BTDM/Zn^{2+} = 1.0) was added to the mixture under fast magnetic stirring at RTP. After stirring for 1 min, the obtained precipitate was filtered, and activated in ethanol solution (four times) at 60°C for a total duration of 48 h, then dried overnight in an oven at 120°C. The resulting product is denoted as H-ZIF-90_A1. The procedure used to synthesize H-ZIF-90_B1 was similar to the procedure used to prepare H-ZIF-90_A1, except that the template BTDM was replaced by TMPDA.

Table S1. Chemical structures of template used in this work and their corresponding abbreviations.

Template	Structure Formula	Abbreviation
1, 4-butanediamine	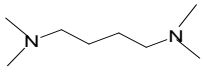	BTDM
tetramethyl-1, 3-propanediamine	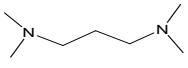	TMPDA
tetramethyldiaminomethane	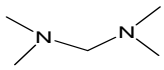	TMDT

Table S2. Porosity properties and STYs of the as-synthesized H-MOFs.

Sample	S_{BET}[$m^2 \cdot g^{-1}$][a]	S_{meso}[$m^2 \cdot g^{-1}$][b]	V_t[$cm^3 \cdot g^{-1}$][c]	V_{meo} [$cm^3 \cdot g^{-1}$][d]	STY[$kg \cdot m^{-3} \cdot d^{-1}$][e]
H-HKUST-1_A1	1209	148	0.76	0.36	7.4×10^4
H-HKUST-1_A2	819	136	0.45	0.14	5.4×10^4
H-HKUST-1_A3	759	91	0.37	0.12	5.1×10^4
H-HKUST-1_A1-1	1048	200	0.56	0.16	6.7×10^4
H-HKUST-1_A1-2	1163	177	0.52	0.14	7.7×10^4
H-HKUST-1_A1-3	979	152	0.52	0.20	7.9×10^4
H-HKUST-1_A1-Y	371	41	0.17	0.04	/

[a]BET surface area is calculated by applying the Brunauer–Emmett–Teller (BET) equation; [b]S_{meso} is mesopore surface area; [c]V_t is the total pore volume; [d]V_{meso} is the mesopore volume; [e]Space–time yield (STY) is calculated based on the mass of active products; [f]Commercial HKUST-1 sample, data from Ref.[3]; [g]Record STY for hierarchically structured HKUST-1 synthesized by direct mixing of reactants at 20 × concentration, data from Ref.[4].

Table S3. The C-HKUST-1, H-HKUST-1_A1 and H-HKUST-1_A1-Y samples were characterized by elemental microanalysis (the proper formula of MOF is $Cu_3(BTC)_2(H_2O)_3$).[5]

Sample	C (wt. %)	H (wt. %)	N (wt. %)
C-HKUST-1	32.31	1.87	0.00
H-HKUST-1_A1	26.00	3.91	0.52
H-HKUST-1_A1-Y	34.69	3.50	7.53

Table S4. Binding energy of the Cu^{2+} with ligand and various organic amines.

	Binding energy (kJ/mol)			
	H_3BTC	BTDM	TMPDA	TMDT
Cu^{2+}	-0.928	-0.787	-0.772	-0.742

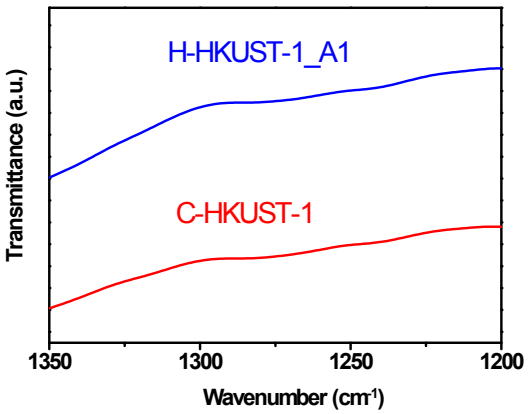

Figure S1. FTIR spectra of H-HKUST-1_A1 and C-HKUST-1 samples in the narrow region of 1340–1210 cm^{-1}.

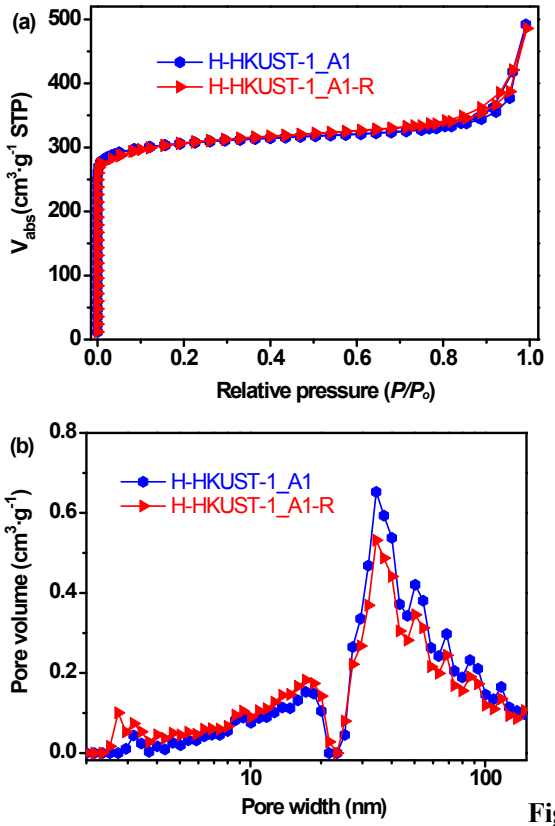

Figure S2. (a) N_2 adsorption–desorption isotherms and (b) pore size distributions (PSDs) of H-HKUST-1_A1 and H-HKUST-1_A1-R (repeated experiment).

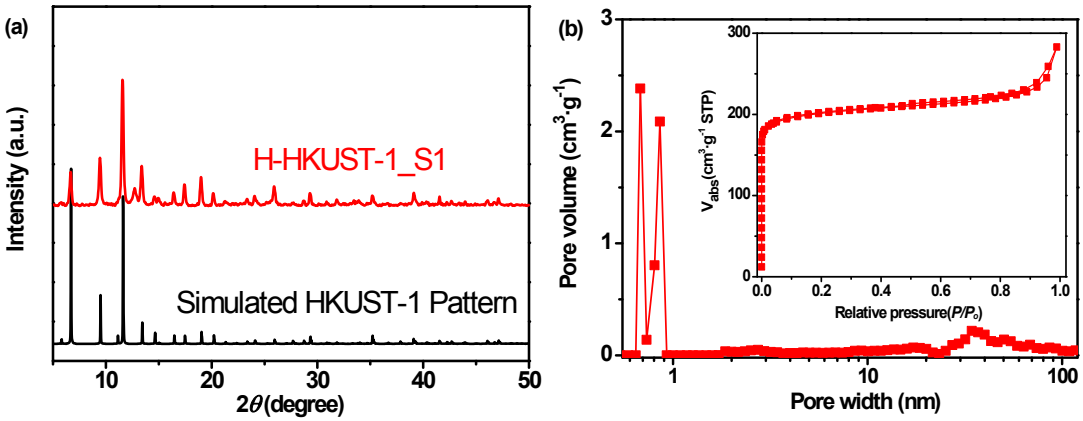

Figure S3. (a) Powder XRD patterns and (b) pore size distributions of H-HKUST-1_S1 sample.

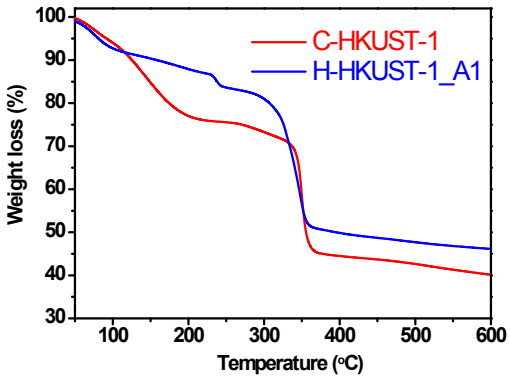

Figure S4. Thermogravimetric analysis (TGA) of H-HKUST-1_A1 and C-HKUST-1.

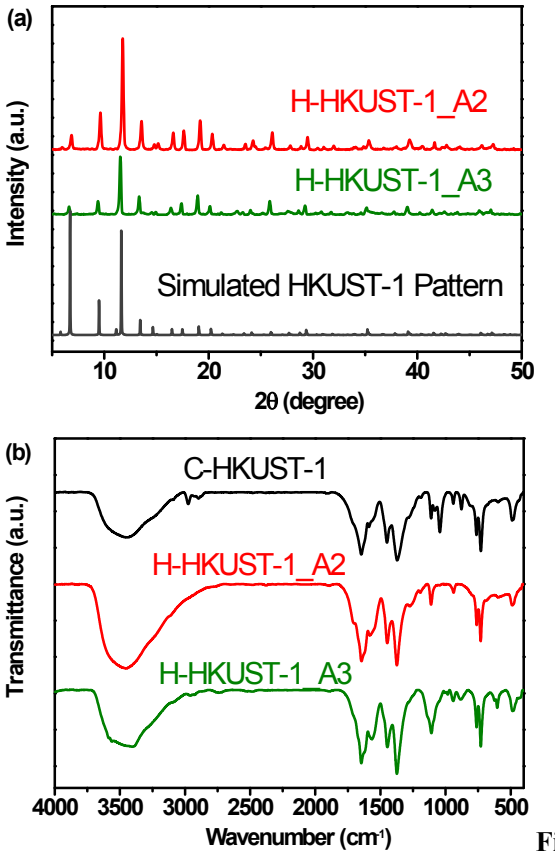

Figure S5. (a) Powder XRD patterns of H-HKUST-1_A*n* (*n* = 2, 3) and the simulated HKUST-1 pattern; (b) FTIR spectra of H-HKUST-1_A*n* (*n* = 2, 3) and C-HKUST-1.

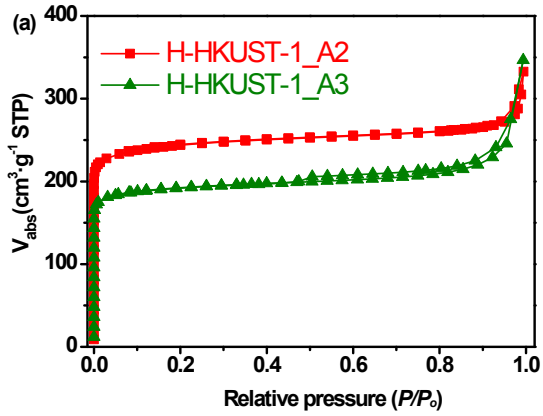

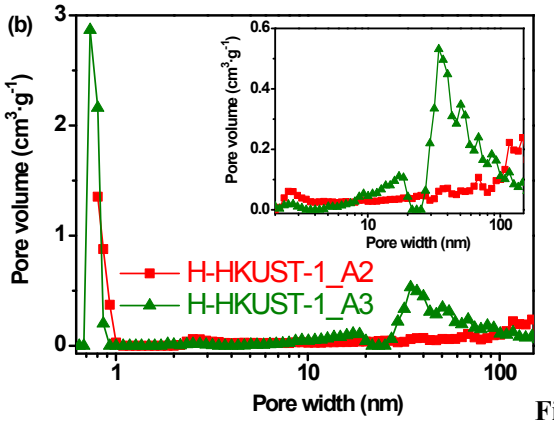

Figure S6. (a) N_2 adsorption–desorption isotherms and (b) pore size distributions (PSDs) of H-HKUST-1_A*n* (*n* = 2, 3).

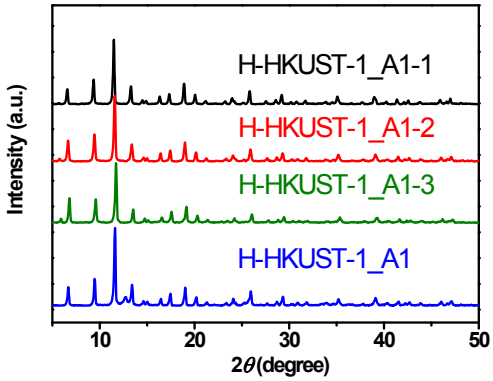

Figure S7. Powder XRD patterns of H-HKUST-1_A1-*m* (*m* = 1, 2, 3) and H-HKUST-1_A1.

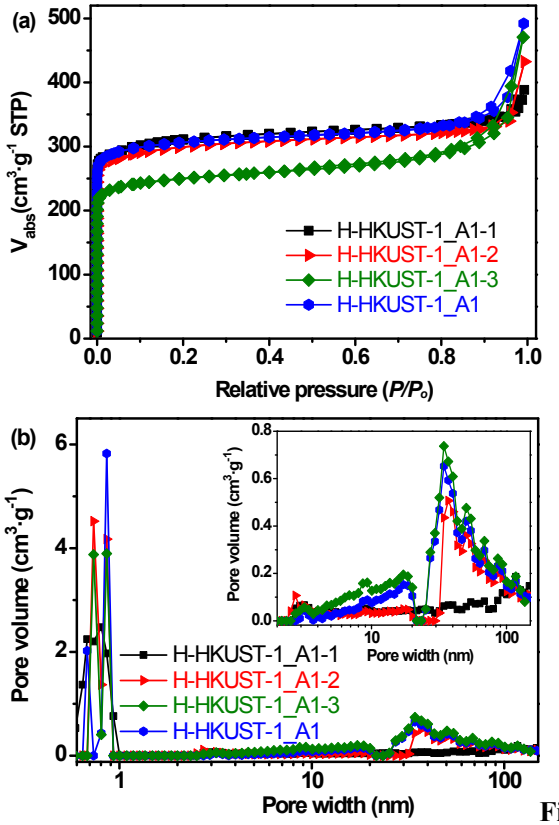

Figure S8. (a) N_2 adsorption–desorption isotherms and (b) PSDs of H-HKUST-1_A1-*m* (*m* = 1, 2, 3) and H-HKUST-1_A1.

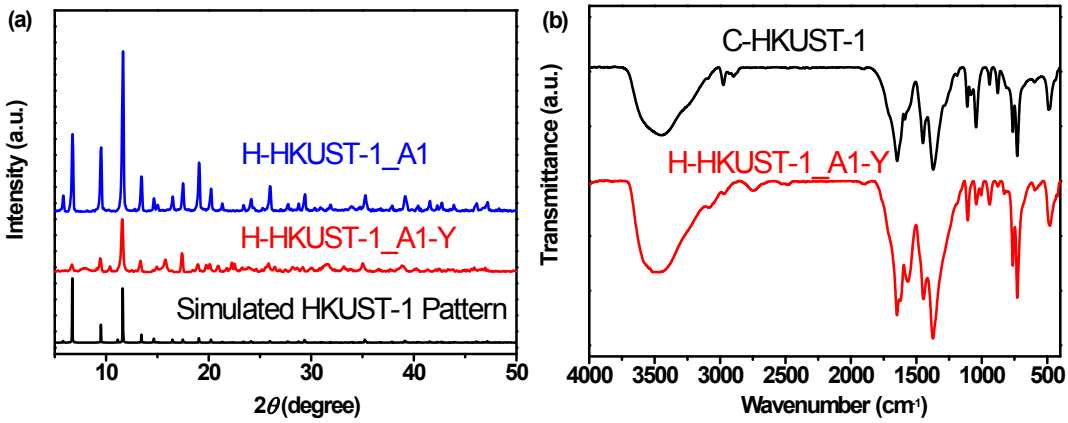

Figure S9. (a) Powder XRD patterns of H-HKUST-1_A1-Y and H-HKUST-1_A1, and the simulated HKUST-1 pattern; (b) FTIR spectra of H-HKUST-1_A1-Y and C-HKUST-1.

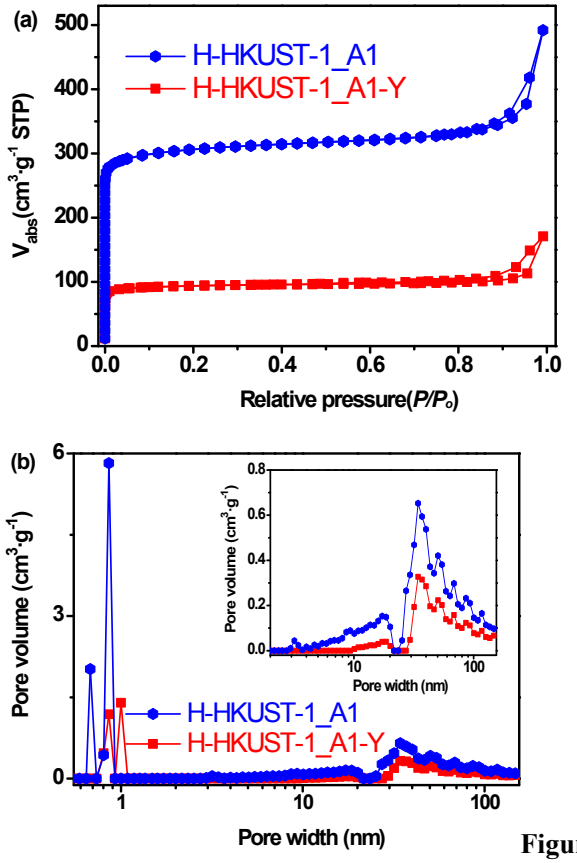

Figure S10. (a) N_2 adsorption–desorption isotherms and (b) PSDs of H-HKUST-1_A1 and H-HKUST-1_A1-Y.

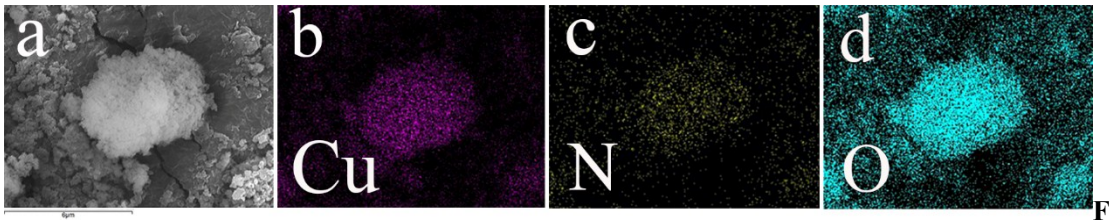

Figure S11. Elemental distribution maps of H-HKUST-1_A1-Y: SEM (a), C (b), N (c), and O (d).

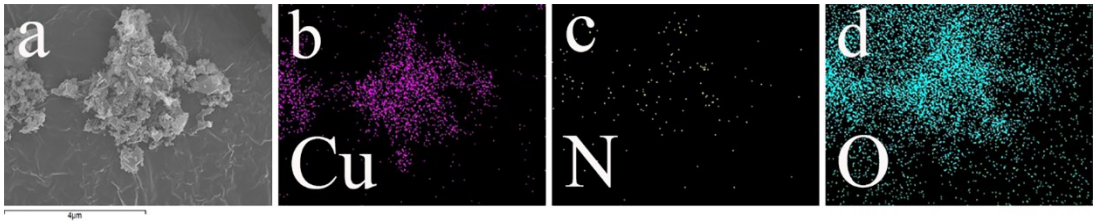

Figure S12. Elemental distribution maps of H-HKUST-1_A1: SEM (a), C (b), N (c), and O (d).

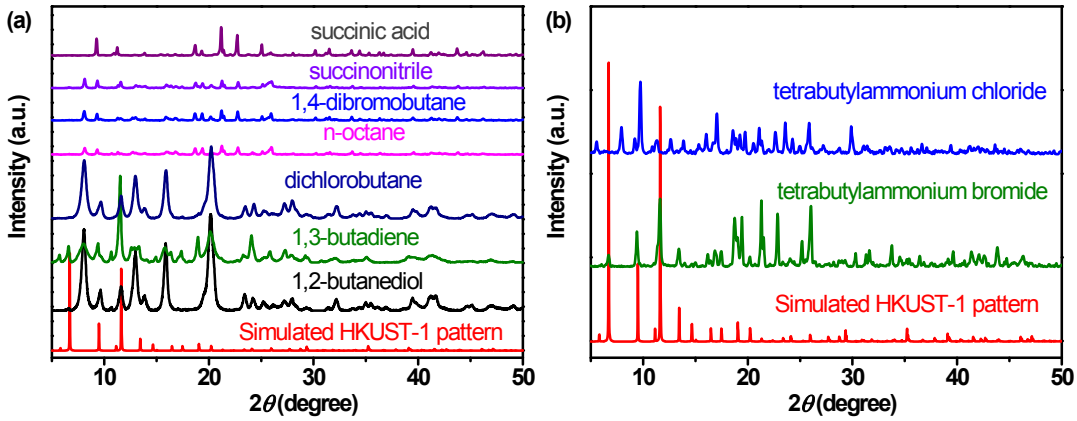

Figure S13. Powder XRD patterns of the obtained products synthesized with different organic molecule (a) and ammonium salts (b) as the templates, respectively, and the simulated XRD pattern.

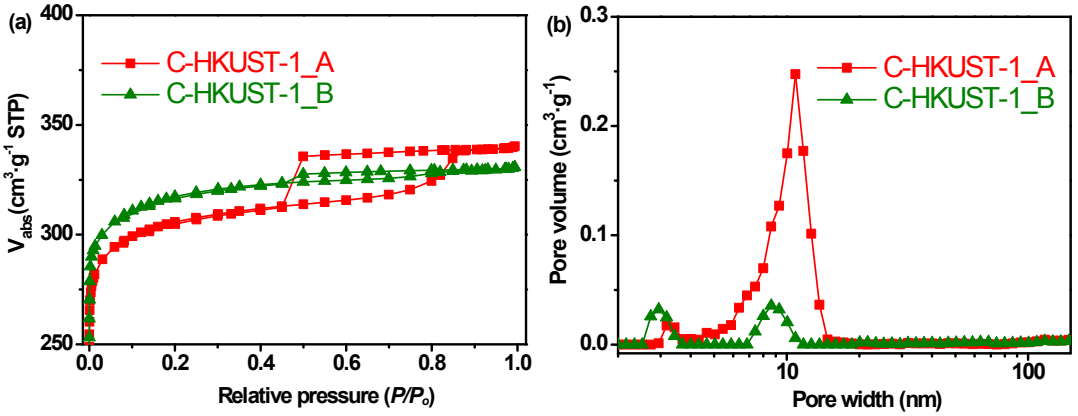

Figure S14. (a) N_2 adsorption-desorption isotherms and (b) PSDs of C-HKUST-1_A and C-HKUST-1_B H-MOFs synthesized within 24 h at 110°C.

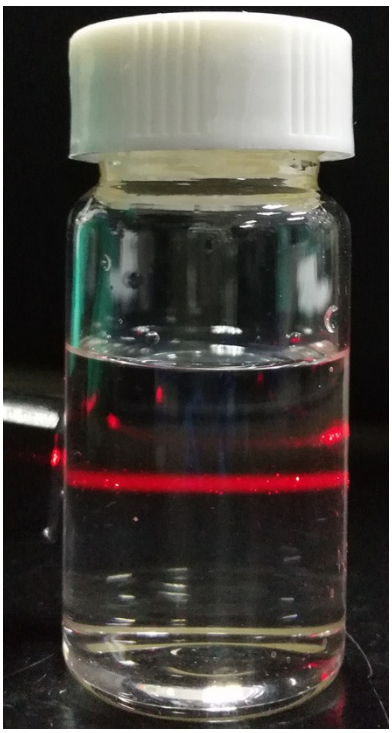

Figure S15. Tyndall scattering effect in the colloidal suspension of BTDM (when laser light is passed through the mixture).

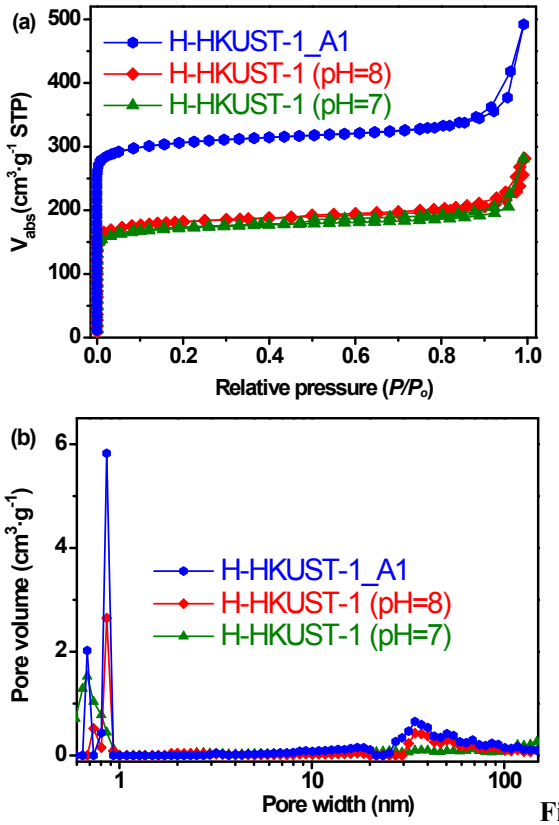

Figure S16. (a) N_2 adsorption-desorption isotherms and (b) PSDs of H-HKUST-1_A1 and H-HKUST-1 H-MOFs synthesized with different pH values (pH =7 and 8), respectively.

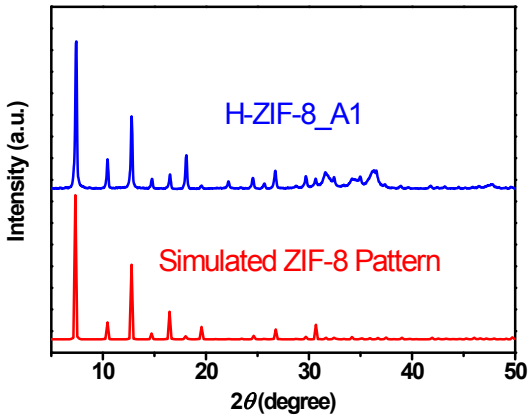

Figure S17. Powder XRD patterns of H-ZIF-8_A1 and the simulated pattern of a single ZIF-8 crystal.

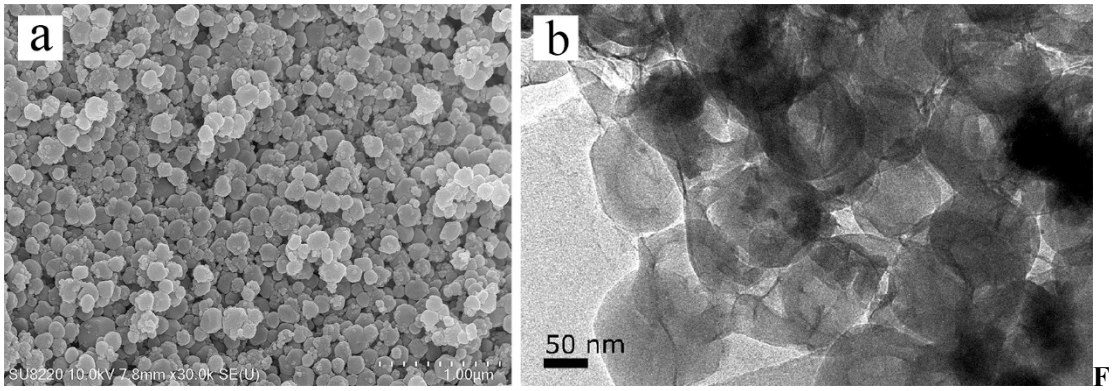

Figure S18. (a) SEM and (b) TEM images of H-ZIF-8_A1 synthesized with BTDM as a template.

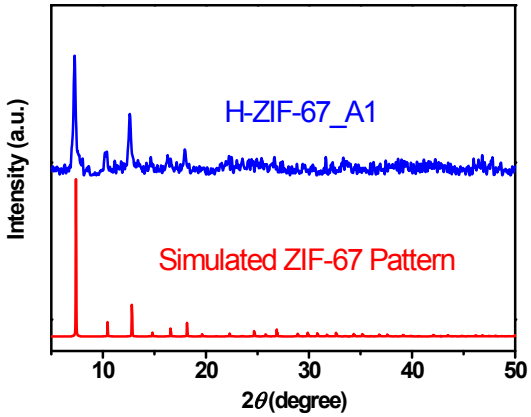

Figure S19. Powder XRD patterns of H-ZIF-67_A1 and the simulated ZIF-67 XRD pattern.

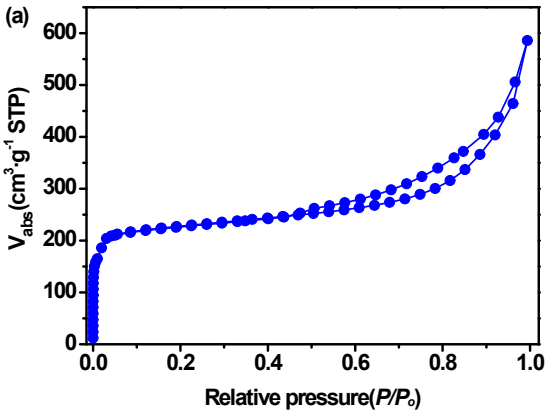

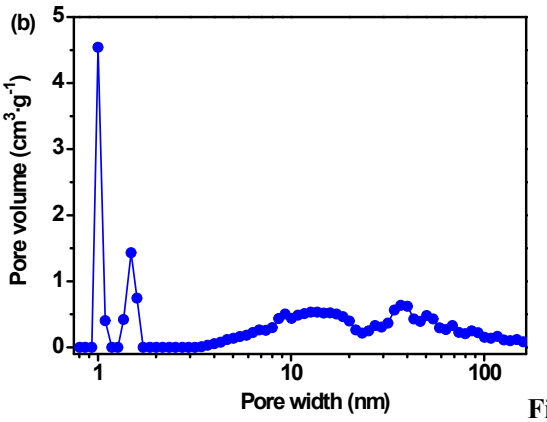

Figure S20. N_2 adsorption–desorption isotherms and PSDs of H-ZIF-67_A1.

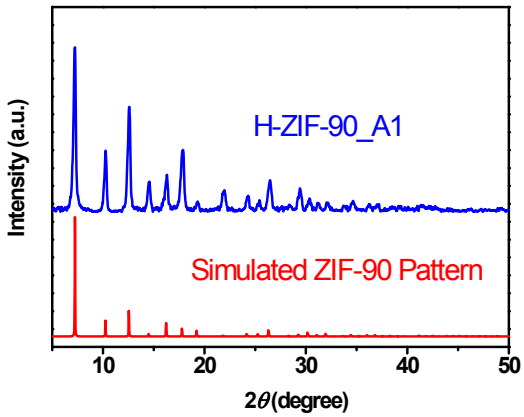

Figure S21. Powder XRD patterns of H-ZIF-90_A1 and the simulated ZIF-90 XRD pattern.

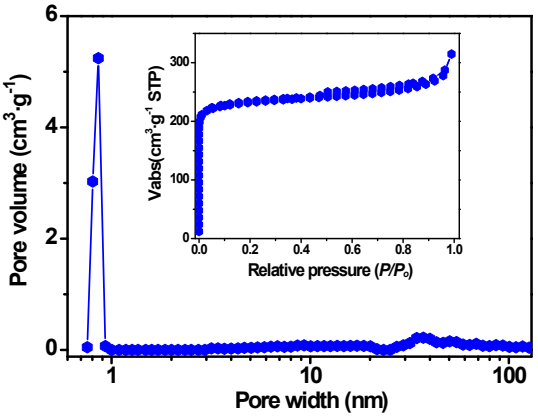

Figure S22. The N_2 adsorption–desorption isotherms and PSDs of H-ZIF-90_A1.

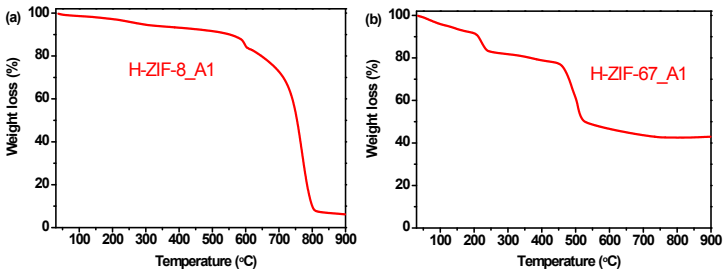

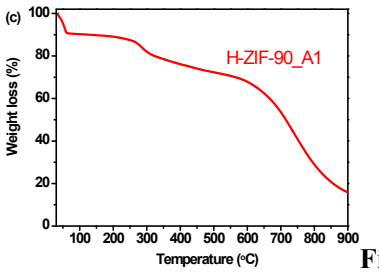

Figure S23. Thermogravimetric analysis (TGA) of H-MOFs: (a) H-ZIF-8_A1; (b) H-ZIF-67_A1, and (c) H-ZIF-90_A1.

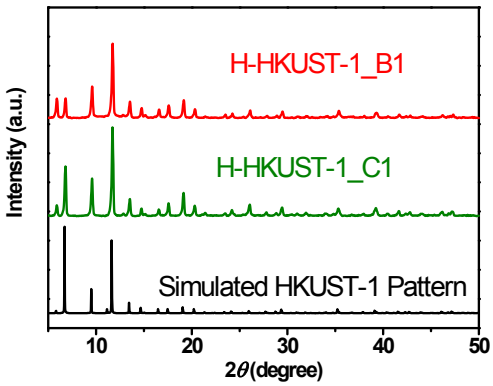

Figure S24. Powder XRD patterns of H-HKUST-1_*X*1 (*X* = B, C) and the simulated HKUST-1 pattern.

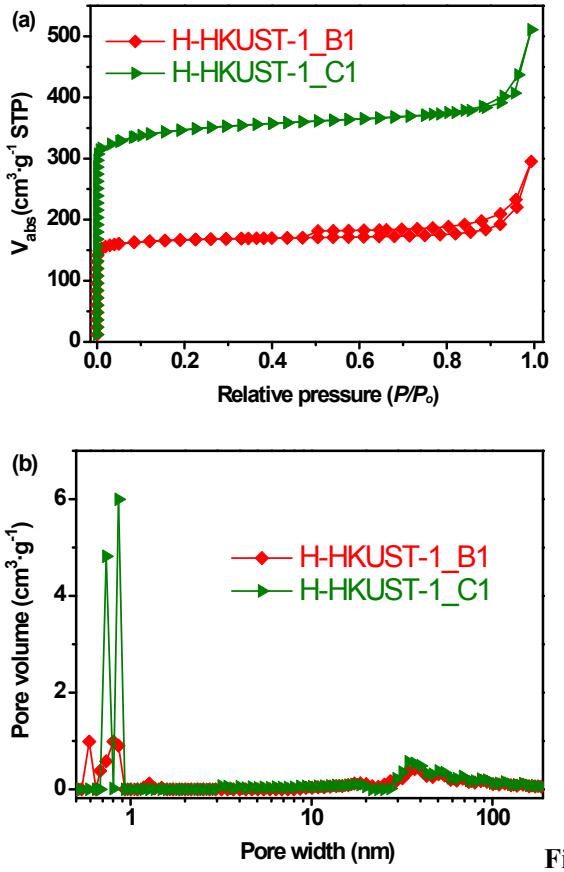

Figure S25. N_2 adsorption-desorption isotherms and PSDs of H-HKUST-1: (a) H-HKUST-1_B1; (b) H-HKUST-1_C1.

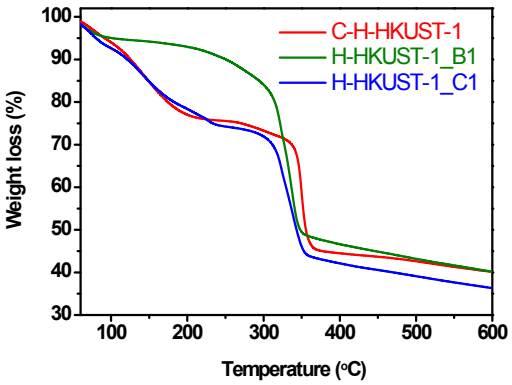

Figure S26. TGA of H-HKUST-1_*X*1 (*X* = B, C) and C-HKUST-1 samples.

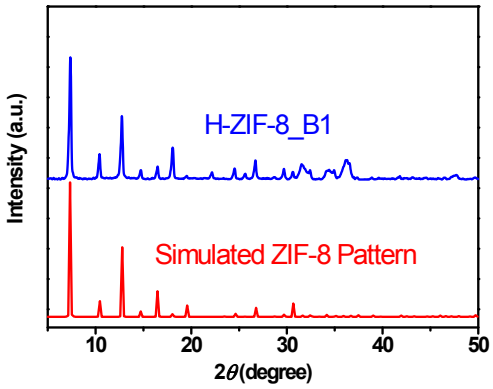

Figure S27. Powder XRD patterns of H-ZIF-8_B1 and the simulated ZIF-8 XRD pattern.

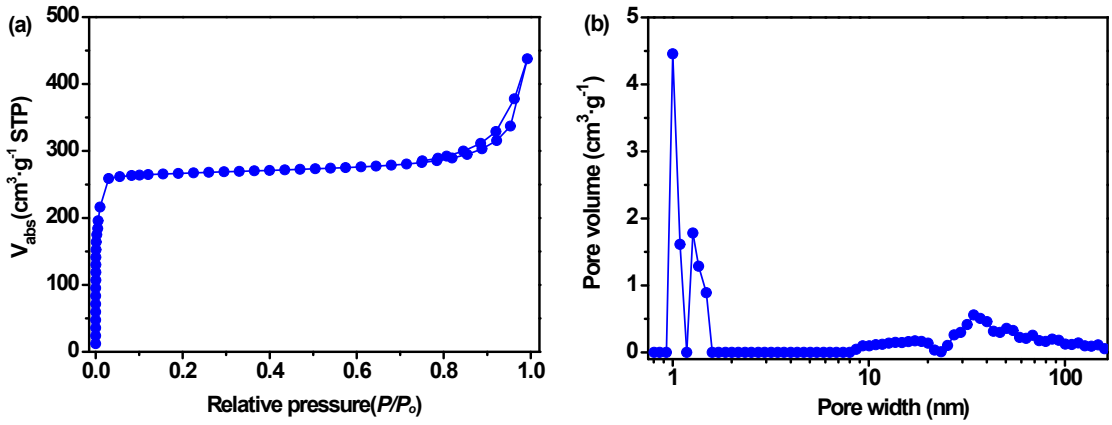

Figure S28. (a) N_2 adsorption-desorption isotherms and (b) PSD of H-ZIF-8_B1 sample**.**

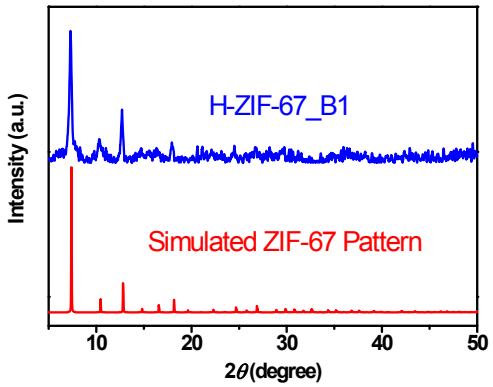

Figure S29. Powder XRD patterns of H-ZIF-67_B1 and the simulated ZIF-67 XRD pattern.

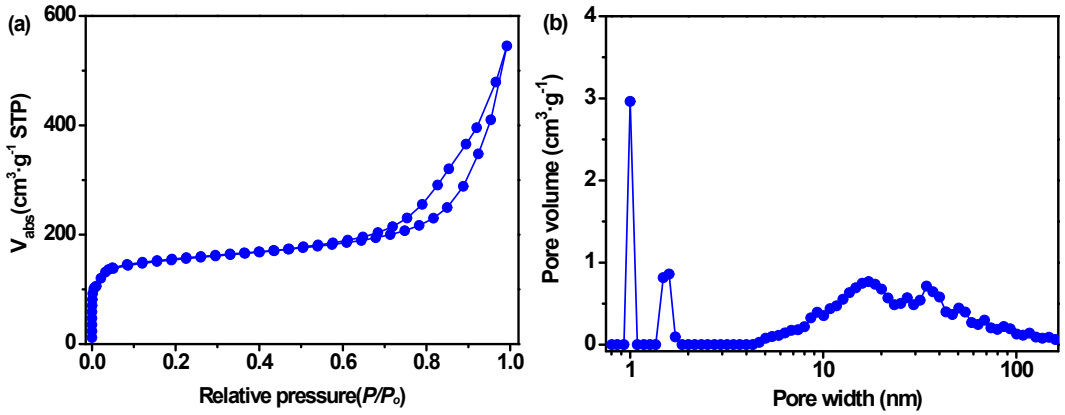

Figure S30. (a) N_2 adsorption-desorption isotherms and (b) PSD of H-ZIF-67_B1.

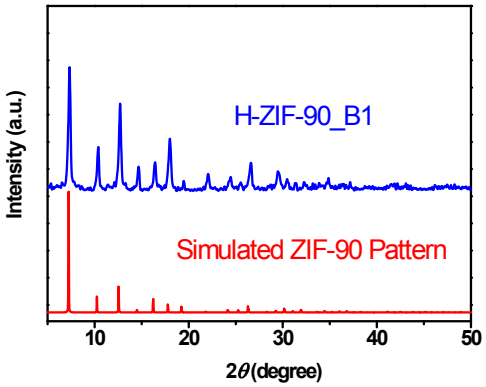

Figure S31. Powder XRD patterns of H-ZIF-90_B1 and the simulated ZIF-90 pattern.

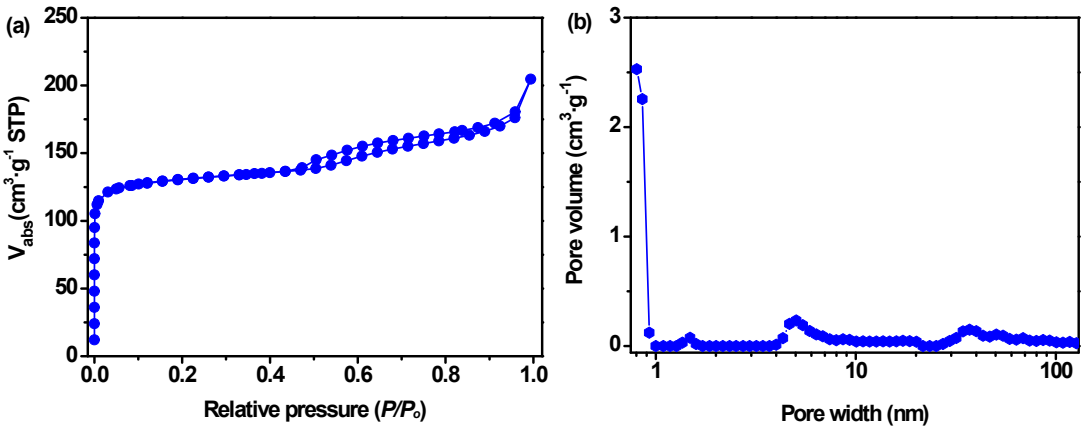

Figure S32. The N_2 adsorption-desorption isotherms and PSD of H-ZIF-90_B1.

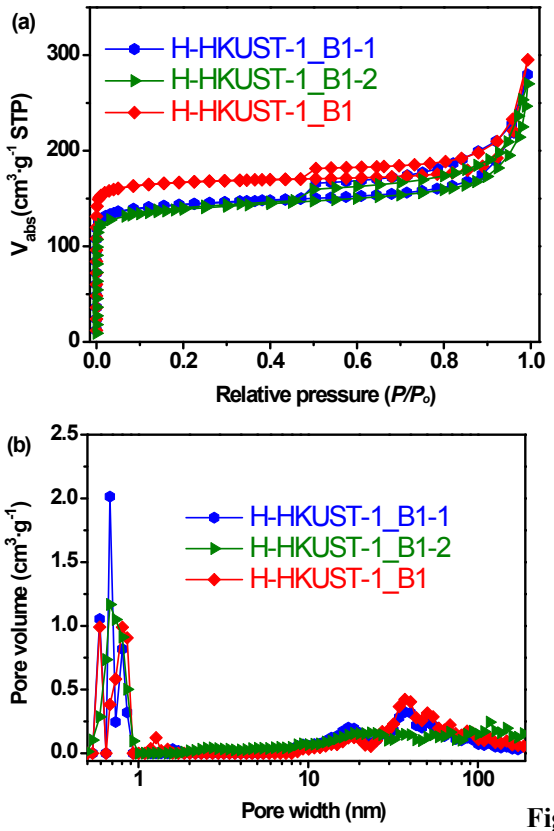

Figure S33. (a) N_2 adsorption–desorption isotherms and (b) PSDs of H-HKUST-1_B1 and H-HKUST-1_B1-m (*m* = 1, 2, where *m* represents the amount of TMPDA, *i.e.*, *m* = 1 for 2.25 mmol, and *m* = 2 for 9.0 mmol).

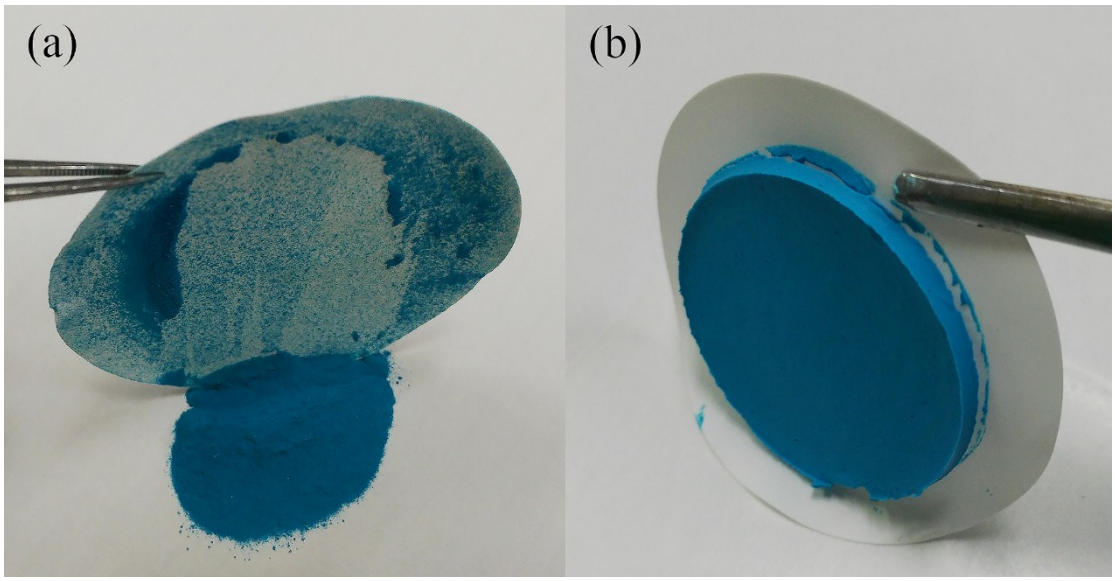

Figure S34. The macromorphology of (a) C-HKUST-1 and (b) H-HKUST-1_A1 materials.

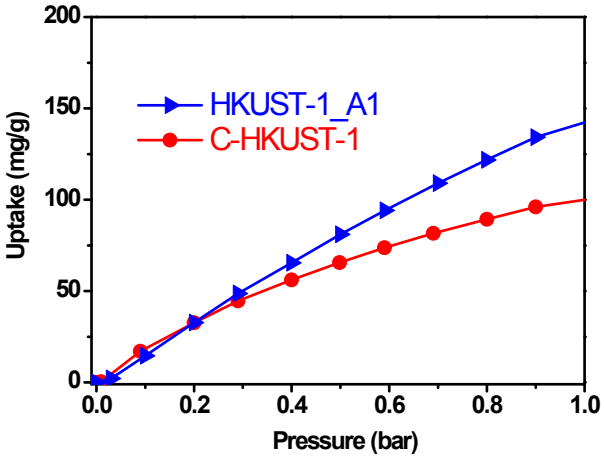

Figure S35. CO_2 adsorption isotherms of H-HKUST-1_A1 and C-HKUST-1 at 298.15 K.

References

1. S.S.-Y. Chui, S.M.-F. Lo, J.P. Charmant, A.G. Orpen, I.D. Williams, *Science* 283 (1999) 1148-1150.

2. A.F. Gross, E. Sherman, J.J. Vajo, *Dalton T.,* 41 (2012) 5458-5460.

3. A.U. Czaja, N. Trukhan, U. Muller, *Chem. Soc. Rev.,* 38 (2009) 1284-1293.

4. J. Huo, M. Brightwell, S. El Hankari, A. Garai, D. Bradshaw, *J. Mater. Chem. A*, 1 (2013) 15220-15223.

5. S. Cao, G. Gody, W. Zhao, S. Perrier, X. Peng, C. Ducati, D. Zhao, A.K. Cheetham, *Chem. Sci.,* 4 (2013) 3573.